Optimization Methods to Plan the Charging of Electric Vehicle Fleets

Olle Sundström and Carl Binding
IBM Research, Zurich, 8803 Rüschlikon, Switzerland
Email: {osu, cbd}@zurich.ibm.com

***Abstract*—This paper describes an approach to optimize electric vehicle battery charging behavior with the goal of minimizing charging costs, achieving satisfactory state-of-energy levels, and optimal power balancing. Two methods for charging schedule optimization are compared. The first formulation uses a linear approximation of the battery behavior, whereas the second uses a quadratic approximation. A non-linear and state-dependent battery model is used to evaluate the solutions of the two methods. Our results indicate that the linear approximation is sufficient when considering the electric vehicle charging plan optimization.**

***Index Terms*—Electric Vehicles, Balancing Power, Electricity Grid, Intermittent Energy Sources, Smart Charging, Distribution Networks, Demand Management**

I. Introduction

The automotive industry is heavily investing in plug-in hybrid elecrical vehicles (PHEV) as well as fully electric vehicles (EV) mainly to address the CO_2 emissions and oil dependency of current automotive technology. The first commercial models are expected to appear on the markets soon; predictions regarding their commercial success however vary [1].

One aspect to consider is that with large PHEV and EV[1] fleets the electrical grids may have to cope with additional loads that exhibit different characteristics than household appliances [2]. The impact of EV fleets was studied in the literature as early as 1983 with a study on the timing of EV recharging and its effect on utilities [3]. Rahman et al. [4] have anticipated the implications of EVs on power distribution grids. They point to the importance of the effects of large EV fleets on the distribution grid, new load peaks in time slots of previously weak demand, and the effects of long charging cycles of batteries; see also [2]. Koyanagi et al. [5] propose time-shifted fast charge at lunch and night time to avoid peak loads in the time intervals that already experience heavy loads. A summary energy usage model for EVs is used. The impact of a fleet of EVs on the Vermont power grid has been studied in [6]. Assuming a dual-tariff, nightly charging scheme, the authors conclude that sufficient transport and distribution capacities are available in the power grid. More details on potential low-voltage distribution grid impacts are given in [7].

Several investigations are also under way that study the use of a fleet of EVs to provide services to the electrical grid. Such concepts are commonly known as vehicle-to-grid (V2G) concepts. By using controlled charging, and possibly controlled discharging, of a large number of EV accumulators, it is hoped that peaks and troughs of electrical power generation can be conveniently absorbed by providing balancing power. To have an EV fleet enter the balancing power market, a large number of such loads has to be aggregated and managed [8].

Providing balancing power is especially important for electrical grids with a high percentage of intermittent energy resources, such as photo-voltaic or wind. Fleets of EVs may be used to supply short-term balancing power to equilibrate power generation and consumption - thus becoming beneficial to the grid's operation.

The potential economic impact of such a large-scale V2G integration has been analyzed by Kempton et al. in [9]. The economics presented there become even more relevant in grids with large amounts of wind energy as described in [10], [11], taking into account the economics of balancing power required for highly intermittent energy sources.

The overall problem can be seen as a suitable planning and execution of power generation and consumption schedules to satisfy high-volume balancing as well as low-volume, car charging power requirements. The goals for the various parties that are involved are as follows: reduced requirements for costly balancing power, avoidance of transport and distribution grid bottlenecks, and satisfaction of end-user needs, i.e., a sufficient charging level in the EV must be reached. These goals can be addressed by establishing a *charging plan* for each EV in the system. Such plans are akin to the traditionally known power generation schedules used in the power generation community, but with a much smaller energy volume. These charging plans should be determined using predictions of the trip characteristics for the next planning period.

In establishing such a charging plan, the vehicle's battery plays an important role. Its charging and discharging behavior has to be accounted for in the planning by deriving expected energy consumpution values. Non-linearities in the relationship between applied, external, charging power and the rate of change of the battery's state-of-energy, i.e., the internal power have to be considered. This paper presents a comparisons of the resulting charging plans when using two different approximations of the non-linear battery behavior. This is done in order to quantify the level of detail necessary in the optimization for establishing the charging plan.

The remainder of this paper is organized as follows. Sec-

[1]We shall use, from now on, the term EV to denote either PHEV or full EV, unless such distinction is relevant.

tion II contains the modelling of EV battery. Section III discusses the methods used to optimize the EV battery charging. The comparison of different battery types and optimization methods is given in Section IV. Finally, Section V summarizes our findings and gives an outlook of further work in the area.

II. Electric Vehicle Model

From the charging planning perspective the EVs are considered to be battery packs in this study, that have non-linear behavior. Each battery is modeled as an equivalent electric circuit containing a voltage source in series with a resistor. Both the voltage source and the internal resistance are dependent on the state-of-energy ζ of the battery. The battery parameters also depend on the specific cell charateristics and the size of the battery pack. This type of battery model is commonly used when considering the supervisory control of hybrid electric vehicles [12]. The model therefore suits the purpose of supervisory control of the charging of EVs well. Based on the equivalent circuit the battery current is derived as a function of the state-of-energy and the input, or output, power P_b (positive during charging) to the battery

$$I_b(\zeta, P_b) = \frac{V_{oc}(\zeta) - \sqrt{V_{oc}(\zeta)^2 + 4R_{int}(\zeta)P_b}}{2R_{int}(\zeta)}. \quad (1)$$

The output voltage is a function of the state-of-charge and the input or output power

$$V_b(\zeta, P_b) = V_{oc}(\zeta) - I_b(\zeta, P_b)R_{int}(\zeta). \quad (2)$$

Because of battery limitations, the output voltage must be within the given voltage limitations

$$V_b(\zeta, P_b) \in [V_{min},\ V_{max}]. \quad (3)$$

However, the voltage limitations can be seen as state-of-energy-dependent current limitations

$$I_b(\zeta, P_b) \in \left[\frac{V_{oc}(\zeta) - V_{max}}{R_{int}(\zeta)},\ \frac{V_{oc}(\zeta) - V_{min}}{R_{int}(\zeta)}\right]. \quad (4)$$

The battery current must also be within the static current limitations given by the manufacturer

$$I_b(\zeta, P_b) \in [-I_{max},\ I_{max}]. \quad (5)$$

The only dynamic state variable for a single vehicle is the state-of-energy $\zeta \in [0,\ 1]$. The change in state-of-energy is the internal battery power over the maximum stored energy in the battery

$$\dot{\zeta} = f(\zeta, P_b) = \frac{P_{int}(\zeta, P_b)}{E_{int0}}, \quad (6)$$

where the maximum stored energy in the battery is

$$E_{int0} = \int_0^1 V_{oc}(\zeta)Q_0\ d\zeta \quad (7)$$

and the internal power of the battery is

$$P_{int}(\zeta, P_b) = \begin{cases} -\eta I_b(\zeta, P_b)V_{oc}(\zeta) & P_b \geq 0 \\ -\frac{1}{\eta} I_b(\zeta, P_b)V_{oc}(\zeta) & P_b < 0. \end{cases} \quad (8)$$

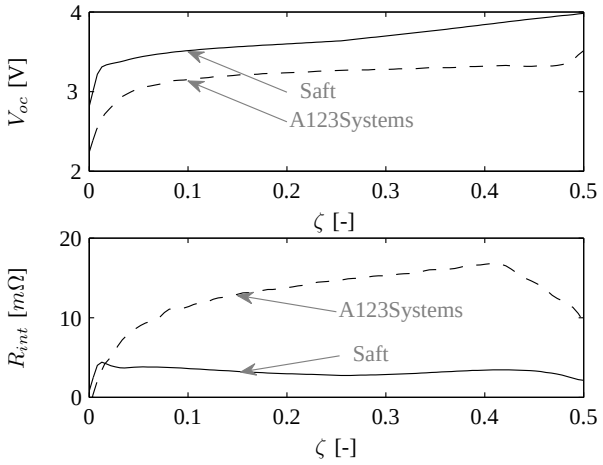

Figure 1. The open circuit voltage and internal resistance of the Saft VL 45E cell and of the A123Systems 26650 cell.

Table I
Parameters of the VL 45E cell and of the 26650 cell.

Variable	VL 45E	26650	Unit	Scaling
E_{int0}	590.4	26.5	kJ	$E_{int0} \cdot n_p \cdot n_s$
Q_0	45.0	2.3	Ah	$Q_0 \cdot n_p$
V_{max}	4.0	3.6	V	$V_{max} \cdot n_s$
V_{min}	2.7	2.1	V	$V_{min} \cdot n_s$
I_{max}	100	70	A	$I_{max} \cdot n_p$
$V_{oc}(\zeta)$	see Fig. 1	see Fig. 1	V	$V_{oc}(\zeta) \cdot n_s$
$R_{int}(\zeta)$	see Fig. 1	see Fig. 1	Ω	$R_{int}(\zeta) \cdot \frac{n_s}{n_p}$
$\frac{\partial \eta}{\partial c}$	-167.2	-12.6	s	$\frac{\partial \eta}{\partial c}$

The efficiency is a function of the battery current

$$\eta = 1 + \frac{\partial \eta}{\partial c} \cdot \frac{|I_b(\zeta, P_b)|}{Q_0}, \quad (9)$$

where $\frac{\partial \eta}{\partial c}$ is a constant reflecting the decrease in efficiency with increasing current. In [13], it was concluded that extreme deviations in the battery state-of-charge are correlated to the ageing of the battery. Typically, the battery operation is therefore limited to a given state-of-charge operating range. Hence, in this paper the state-of-energy is limited to

$$\zeta \in [0.2,\ 0.9]. \quad (10)$$

To investigate the impact of the optimization methods on the actual energy level in the battery, two different battery cells are used. Figure 1 and Table I show the datasheet parameters for the Saft VL 45E [14] and the A123Systems 26650 cell [15]. The parameters E_{int0}, $V_{oc}(\zeta)$, $R_{int}(\zeta)$, and $\frac{\partial \eta}{\partial c}$ have been identified using the model in (1)–(10) and using information on the datasheets [14], [15].

The battery pack for each vehicle is scaled according to the scaling equations in Table I. Note that the scaling variables n_s and n_p are not necessarily integers. Consequently, the resulting battery pack after scaling may not be implementable in a vehicle. It is however assumed that the behavior of the pack reflects the real behavior sufficiently well.

The EV fleet comprises two types of vehicles, namely, commuter vehicles and taxi vehicles. In this paper, the EV

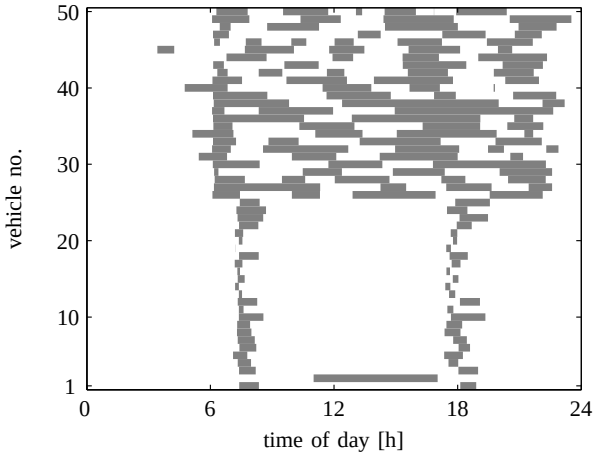

Figure 2. The time each vehicle is available for smart charging (white) and the time each vehicle is unplugged (gray). The values are given for the day considered. Vehicles 1-25 are commuter vehicles, and vehicles 26-50 are taxis.

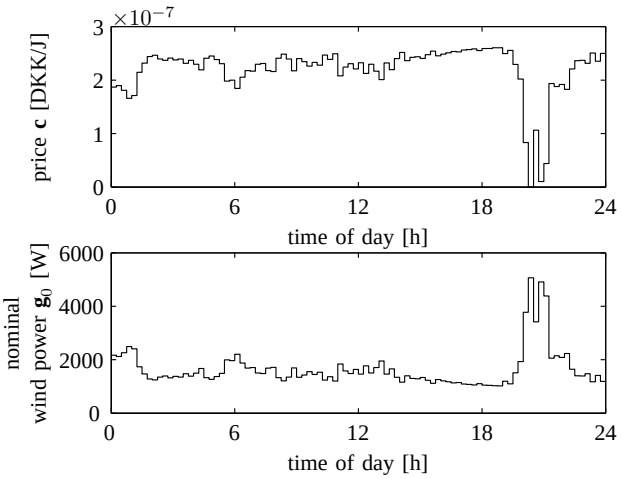

Figure 3. The top graph shows the assumed price curve on the considered day. The bottom graph shows the assumed wind power potential.

fleet is assumed to contain equal shares of commuter and taxi vehicles. The usable energy capacity of the battery is the energy between the state-of-energy limits in (10). The taxi vehicles have an energy capacity of 36.8 kWh, and the commuter vehicles have an energy capacity of 18.4 kWh, both with a nominal voltage of 400 V.

As the actual energy requirement the next day is unknown at the time of planning, the behavior of the EVs has to be predicted. The focus of this paper is not on driving pattern prediction. However, it is assumed that the driving pattern prediction has already been done and that the following information is available for the predicted stop-over k for vehicle i:

- time of connection $t_{c,i,k}$
- time of disconnection $t_{d,i,k}$
- energy required for the next trip $E_{i,k}$.

In addition to the information above, a predicted energy content E_0 in the battery at midnight, when the day begins, is assumed to be known.

Note that the energy goals and times of connection and disconnection can either be set explicitly by the end-user or, as assumed in this paper, predicted using historical data. For example, the energy level to be reached can reflect an average or weighted average level as well as an extreme[2] energy goal.

Figure 2 shows the time of connection and time of disconnection for each stop-over (white area) for a fleet of 50 vehicles. The gray areas in Fig. 2 represent the trip durations. It clearly shows the differences between the taxi and the commuter vehicles. The latter have a low number of trips at relatively fixed times, whereas the former have a more irregular pattern.

III. Optimization Methods

Throughout this paper it is assumed that both the price of electricity and the available wind power are predicted and known for the next planning period. The optimization objective is to minimize the overall cost of charging the EV fleet. Figure 3 shows the assumed price of electricity, $\mathbf{c}$, and the available nominal wind power, $\mathbf{g}_0$. The available wind power is scaled for a fleet with m vehicles using a factor

$$\mathbf{g}_\kappa = \kappa \cdot m \cdot \mathbf{g}_0, \tag{11}$$

where κ is a measure on the excess wind power available.

In this section, two approximations are used to simplify the optimization problem to either a linear program or a quadratically constrained quadratic program.

A. Linear Approximation

Using a linear approximation, the internal power is assumed to be equal to the external power $P_{int} = P_b$. In this case all internal losses in the battery are neglected. The objective is, as mentioned, to minimize the overall cost of charging given the charging constraints and available power constraints. By using the linear approximation for the battery, this problem can be formulated as a linear program:

$$\min_{\mathbf{p}_b} \; t_s \mathbf{c}^T \mathbf{p}_b \tag{12a}$$

subject to

$$\mathbf{A}_s \mathbf{p}_b \;\geq\; \mathbf{b}_s \tag{12b}$$

$$\mathbf{A}_g \mathbf{p}_b \;\leq\; \mathbf{b}_g \tag{12c}$$

$$\mathbf{A}_b \mathbf{p}_b \;\leq\; \mathbf{b}_b \tag{12d}$$

$$\mathbf{b}_l \;\leq\; \mathbf{p}_b \;\leq\; \mathbf{b}_u, \tag{12e}$$

with the cost vector $\mathbf{c}$, the charging power vector $\mathbf{p}_b$, the stop-over inequality constraints ($\mathbf{A}_s$, $\mathbf{b}_s$), the generation inequality constraints ($\mathbf{A}_g$, $\mathbf{b}_g$), the battery inequality constraints ($\mathbf{A}_b$, $\mathbf{b}_b$), and the upper and lower bounds ($\mathbf{b}_u$, $\mathbf{b}_l$). Assume $i = 1, 2..., m$ is the index of the vehicle, $j = 1, 2, ..., n$ the index for the time slot contained in one plan duration. The decision variable $\mathbf{p}_b$ then has $m \cdot n$ elements. Note that all those slots in which no vehicle is connected can be eliminated prior to solving the optimization problem. However, for a reasonably

[2]In this case maximal.

large fleet, it can be assumed that at least one vehicle is connected in each slot. Therefore, the cost vector $\mathbf{c}$ comprises of the cost associated for each vehicle in each time slot $c_{i,j}$. The charging power vector $\mathbf{p}_b$ comprises the charging power for each vehicle and time slot $p_{b,i,j}$.

$$\mathbf{c} = [c_{1,1},\ c_{1,2},\ \ldots,\ c_{1,n},\ \ldots,\ c_{m,1},\ c_{m,2},\ \ldots,\ c_{m,n}]^T \tag{13}$$

$$\mathbf{p}_b = [p_{b,1,1},\ p_{b,1,2},\ \ldots,\ p_{b,1,n},\ \ldots,\ p_{b,m,1},\ p_{b,m,2},\ \ldots,\ p_{b,m,n}]^T. \tag{14}$$

Let the connected duration for a given vehicle i, at a given time slot j, and a given stopover k be

$$d_{i,j,k} \in [0,\ t_s] \tag{15}$$

The connection vector, describing the connection of vehicle i until stopover r, is

$$\mathbf{d}_{i,r} = \left[\sum_{k=1}^{r} d_{i,1,k},\ \sum_{k=1}^{r} d_{i,2,k},\ \ldots,\ \sum_{k=1}^{r} d_{i,n,k}\right]^T. \tag{16}$$

The minimum amount of energy that needs to be charged in vehicle i before the end of stop-over r is

$$E_s(i,r) = -E_0 + \sum_{k=1}^{r} E_{i,k}, \tag{17}$$

where E_0 is the initial energy in the battery at the start of the day. The stop-over inequality constraints are

$$\mathbf{A}_s = [\mathbf{d}_{1,1},\ \mathbf{d}_{1,2},\ \ldots,\ \mathbf{d}_{1,q_1},\ \ldots,\ \mathbf{d}_{m,1},\ \mathbf{d}_{m,2},\ \ldots,\ \mathbf{d}_{m,q_m}]^T \tag{18}$$

$$\mathbf{b}_s = [E_s(1,1),\ E_s(1,2),\ \ldots,\ E_s(1,q_1),\ \ldots,\ E_s(m,1),\ E_s(m,2),\ \ldots,\ E_s(m,q_m)]^T, \tag{19}$$

where q_i is the number of stop-overs for vehicle i.

Let the diagonal matrix with the elements of $\mathbf{d}_{i,q_i}$ on the diagonal be $\mathbf{D}(\mathbf{d}_{i,q_i})$. The generation constraints come from the limited available wind power for each slot

$$\mathbf{A}_g = \frac{1}{t_s}\begin{bmatrix}\mathbf{D}(\mathbf{d}_{1,q_1}) & \mathbf{D}(\mathbf{d}_{2,q_2}) & \cdots & \mathbf{D}(\mathbf{d}_{m,q_m})\end{bmatrix} \tag{20}$$

$$\mathbf{b}_g = \begin{bmatrix}g_{\kappa,1},\ g_{\kappa,2},\ \ldots,\ g_{\kappa,n}\end{bmatrix}^T. \tag{21}$$

Let the maximum amount charged energy for vehicle i before slot j be

$$E_b(i,j) = (0.9 - 0.2)\cdot E_{int0} - E_0 + \sum_{t_{d,j} < t_s \cdot j} E_{i,k}. \tag{22}$$

Let $\mathbf{T}_l(\mathbf{M})$ be the lower triangular matrix of the matrix $\mathbf{M}$. The limited capacity in the batteries results in the battery contraints

$$\mathbf{A}_b = \begin{bmatrix}\mathbf{T}_l(\mathbf{A}_{b,1}) & & & \\ & \mathbf{T}_l(\mathbf{A}_{b,2}) & & \\ & & \ddots & \\ & & & \mathbf{T}_l(\mathbf{A}_{b,m})\end{bmatrix} \tag{23}$$

$$\mathbf{b}_b = \begin{bmatrix}\mathbf{b}_{b,1}^T,\ \mathbf{b}_{b,2}^T,\ \ldots,\ \mathbf{b}_{b,m}^T\end{bmatrix}^T, \tag{24}$$

where $\mathbf{A}_{b,i}$ and $\mathbf{b}_{b,i}$ are

$$\mathbf{A}_{b,i} = \begin{bmatrix}\mathbf{d}_{i,q_i},\ \mathbf{d}_{i,q_i},\ \ldots,\ \mathbf{d}_{i,q_i}\end{bmatrix}^T \tag{25}$$

$$\mathbf{b}_{b,i} = \begin{bmatrix}E_b(i,1),\ E_b(i,2),\ \ldots,\ E_b(i,n)\end{bmatrix}^T. \tag{26}$$

Because of battery, charging spot, or electric grid limitations let the charging power be limited to $\bar{p}_{b,i,j}$. The charging power is then limited to $\mathbf{p}_b \in [0,\ \bar{\mathbf{p}}_b]$.

B. Quadratic Approximation

As the battery in the EV has a non-linear behavior, the next step after using the linear approximation in Section III-A is to approximate the battery using a quadratic function. The actual external power is a non-linear function of the internal power:

$$P_b = f(P_{int}). \tag{27}$$

Approximating this non-linear function using a second-order Taylor series expansion gives

$$P_b = P_{int} + \alpha P_{int}^2, \tag{28}$$

where the term αP_{int}^2 can be seen as the power loss when charging with P_b W. The coefficient α is

$$\alpha(\zeta) = \frac{Q_0 R_{int}(\zeta) - \frac{\partial \eta}{\partial c} V_{oc}(\zeta)}{Q_0 V_{oc}(\zeta)^2}. \tag{29}$$

Assuming a nominal state-of-energy $\zeta_n = 0.5$ gives an approximation for the coefficient $\tilde{\alpha} = \alpha(\zeta_n)$. The corresponding coefficient vector for the decision vector $\mathbf{p}_{int}$ is

$$\tilde{\boldsymbol{\alpha}} = [\tilde{\alpha}_{1,1},\ \tilde{\alpha}_{1,2},\ \ldots,\ \tilde{\alpha}_{1,n},\ \ldots,\ \tilde{\alpha}_{m,1},\ \tilde{\alpha}_{m,2},\ \ldots,\ \tilde{\alpha}_{m,n}]^T, \tag{30}$$

with $\tilde{\alpha}_{i,j} = \tilde{\alpha}_{i,j+1}\ \forall\ j = 1,\ldots,n-1$ because the state-of-energy dependency in the model during the optimization is neglected.

The optimization problem using the quadratic approximation (28) is

$$\min_{\mathbf{p}_{int}}\ t_s \mathbf{c}^T \mathbf{p}_{int} + t_s \mathbf{p}_{int}^T \mathbf{D}(\tilde{\boldsymbol{\alpha}})\mathbf{D}(\mathbf{c})\mathbf{p}_{int} \tag{31a}$$

subject to

$$\mathbf{A}_s \mathbf{p}_{int} \leq \mathbf{b}_s \tag{31b}$$

$$\mathbf{A}_{g,j}\mathbf{p}_{int} + \mathbf{p}_{int}^T \mathbf{D}(\tilde{\boldsymbol{\alpha}})\mathbf{D}(\mathbf{A}_{g,j})\mathbf{p}_{int} \leq g_j\ j = 1,\ldots,n \tag{31c}$$

$$\mathbf{A}_b \mathbf{p}_{int} \leq \mathbf{b}_b \tag{31d}$$

$$\mathbf{p}_{int} \geq \mathbf{b}_l \tag{31e}$$

$$\mathbf{q}_r \mathbf{p}_{int} + \mathbf{p}_{int}^T \mathbf{D}(\tilde{\boldsymbol{\alpha}})\mathbf{D}(\mathbf{q}_r)\mathbf{p}_{int} \leq b_{u,r}\ r = 1,\ldots,mn \tag{31f}$$

where $\mathbf{q}_r$ is the vector with $m \cdot n$ elements, where element r is one and the remaining elements are zeros. Finally, the external power schedule $\mathbf{p}_b$ is calculated using (28).

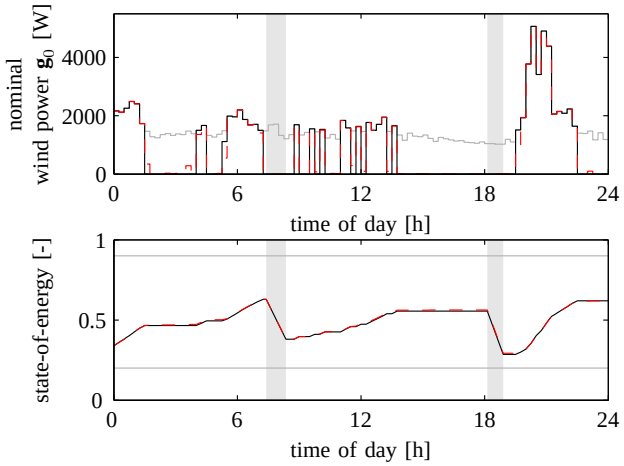

Figure 4. The top graph shows the charging plans when using the linear formulation (black curve), the quadratic formulation (red curve), and the available wind power (gray curve). The bottom graph shows the resulting state-of-energy trajectory when applying both the linear (black) and the quadratic approximation (red). The time the vehicle is unplugged is indicated by gray shadowing.

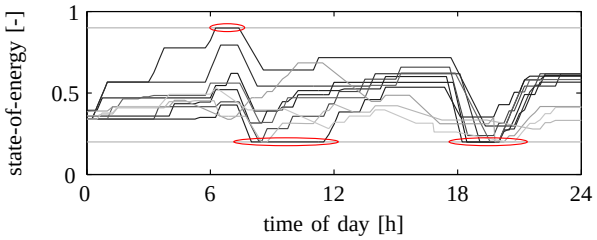

Figure 5. Resulting state-of-energy trajectories of 10 out of 50 vehicles after applying the charging schedule. Critical points are indicated by red circles, where the state-of-energy might violate the boundaries of the battery.

IV. Evaluation and Comparison

The solutions of the two optimization problems in Section III are found using the IBM ILOG CPLEX[3] library [16]. The focus of this section is to show the solutions and to quantify the drawbacks of using the simpler linear approximation. This is done in order to assess the necessity of using higher-order approximations for supervised charging of electric vehicles. The evaluation process in this section is as follows:

1) Calculate the charging schedule (based on the linear or the quadratic approximation in Section III).
2) Apply the charging shedule in an ODE solver of the detailed EV model in Section II.
3) Observe the resulting state-of-energy trajectory and detect *state-of-energy boundary violations*.

Figure 4 shows the solutions to the linear and quadratic optimization problems with the price and wind power profiles in Fig. 3 for vehicle no. 1 in Fig. 2. The top graph of Fig. 4 shows the generated power $\mathbf{g}_\kappa$ with $\kappa = 1$. It also shows the charging schedule determined using the linear approximation (solid black curve) and the charging schedule determined using the quadratic approximation (red dashed curve). The difference between the two charging schedules is minor and indicates that the linear approximation is sufficient. The bottom graph of Fig. 4 shows the resulting state-of-energy trajectories when applying the two charging schedules in the top graph. There is a small, but noticable difference between the state-of-energy trajectories. This effect comes from the fact that the linear approximation neglects all energy losses in the battery, whereas the quadratic approximation includes a quadratic approximation of the losses. The resulting state-of-energy trajectory after applying the schedule based on the linear approximation is therefore lower than the one using the schedule based on the quadratic approximation.

[3]IBM, ILOG and CPLEX are trademarks of International Business Machines Corporation in the United States, other countries, or both. Other product and service names might be trademarks of other companies.

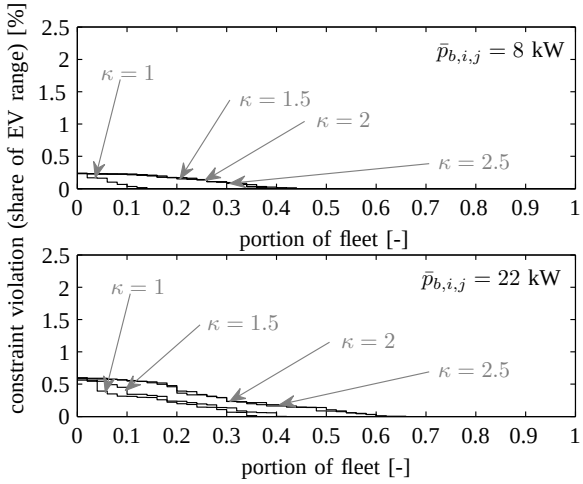

Figure 6. The severity of the battery constraint violation, for the A123Systems 26650 fleet, as a function of the portion of the fleet that violates the battery constraint.

Figure 5 shows the state-of-energy trajectories for a fleet of 50 EVs after applying the schedule based on the linear approximation. The potential issues with the linear approximation can now be observed. Even though the optimization problem is set up to handle the upper and lower state-of-energy boundaries, *violations* of these constraints may occur (red circles) during the execution of the schedule. The actual violations of the state-of-energy boundaries during the execution of the schedules are therefore further analyzed and quantified.

As the losses in the battery, which are the underlying causes of the constraint violations, increase with increasing charging power, it is important to investigate different charging power limitations $\bar{p}_{b,i,j}$ as well as variations in available wind power, i.e., changing κ. The charging power limitation is assumed to be 3.5 kW (for a normal household connection), 8 kW, or 22 kW. In fact, there are no significant constraint violations for the lowest charging power limitation of 3.5 kW. The results are therefore only shown for the higher limitations, i.e., 8, and 22 kW. The constraint violations are given as a share of the total range of the EV, which in fact are equal to the share of the usable state-of-energy range. Figures 6 and 7 show the constraint violations assuming the entire fleet has the A123 Systems battery or the Saft battery, respectively. There are no

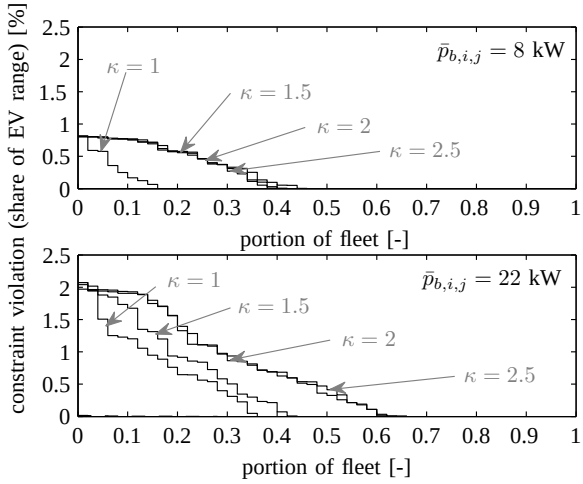

Figure 7. The severity of the battery constraint violation, for the Saft VL45 E fleet, as a function of the portion of the fleet that violates the battery constraint.

Table II
THE INCREASE IN CALCULATION.

EV fleet size	10	20	30	40	50
$t_{\text{calc,quadratic}}/t_{\text{calc,linear}}$	238	338	441	760	819

significant violations when using the quadratic approximation, thus Figs. 6 and 7 only show the results when using the linear approximation. The share of the fleet experiencing violations of the boundaries and the severity of the violations increase with increasing availability of wind power. The reason for this is that the resulting charging schedules, using the linear approximation, are able to utilize higher charging power at times when the price is low. The same effect can be observed when increasing the charging power limitation. Note that there is a difference between the two battery types. The fleet with the Saft battery has a higher share of constraint violations and also experiences larger violations.

Note that in this study the future trip information is assumed to be completely known during planning. This assumption is made to isolate the effects of using a linear approximation for charging schedule optimization. However, the severity of the violations of the battery boundaries when using the schedule based on the the linear approximation is less than 2% of the vehicle range. Even when considering variations in charging power limitation and variations in available wind power, the violations are less that 2%. In reality, the trip information is not known in advance and only predicted trip information will be available. The errors of inperfect trip information are likely to have a significantly larger effect on the violations of the battery boundaries than 2%.

Finally, Table II shows the increase in calculation time when using the quadratic instead of the linear assumption. As the number of constraints is higher and increases faster with a growing fleet in the quadratic formulation than in the linear formulation, the difference in calculation time increases with increasing fleet size. In fact, for a fleet of 50 vehicles, the calculation time using the quadratic formulation is 819 times the calculation time using the linear formulation.

V. CONCLUSION AND FUTURE WORK

In this paper the impact of using a linear versus a quadratic approximation of the EV batteries to plan the charging has been shown. The observation is made that the resulting violations of the battery boundaries when applying the charging schedule based on the linear approximation are relatively small, i.e., less than 2% of the usable capacity. The benefit of using the quadratic formulation does not justify the increase in computation time.

All our optimizations have been based on deterministic optimizations; however most of the inputs to the analyzed system are of random nature. More work is to be done to address the stochastic nature of these phenomena and to validate our estimation and optimzation schemes against real data sets. Another area of interest is to take into account power grid transport and distribution constraints as the optimal charging solution may violate grid constraints.

REFERENCES

[1] P. E. Ross, "Loser: Why the Chevy Volt Will Fizzle," *IEEE Spectrum*, pp. 32–34, January 2010, http://spectrum.ieee.org/magazine/.

[2] P. Farley, "Speed Bumps Ahead for Electric-Vehicle Charging," *IEEE Spectrum*, pp. 13–14, January 2010, http://spectrum.ieee.org/magazine/.

[3] M. M. Collins and G. H. Mader, "The Timing of EV Recharging and Its Effect on Utilities," *IEEE Transactions on Vehicular Technology*, vol. 32, no. 1, pp. 90–97, 1983.

[4] S. Rahman and G. Shrestha, "An Investigation into the Impact of Electric Vehicle Load on the Electric Utility Distribution System," *IEEE Transaction on Power Delivery*, vol. 8, no. 2, pp. 591–597, April 1993.

[5] F. Koyanagi and Y. Uriu, "A Strategy of Load Leveling by Charging and Discharging Time Control of Electric Vehicles," *IEEE Transactions on Power Systems*, vol. 13, no. 3, pp. 1179–1184, 1998.

[6] S. Letendre and R. A. Watts, "Effects of Plug-in Hybrid Electric Vehicles on the Vermont Electric Transmission System," Transportation Research Board Annual Meeting, Washington D.C., January 2009.

[7] J. P. Lopes, F. Soares, and R. R. Almeida, "Identifying Management Procedures to Deal with Connection of Electric Vehicles in the Grid," in *Proceedings of the IEEE Bucharest Power Tech Conference*. IEEE, June 2009.

[8] M. D. Galus and G. Andersson, "Demand Management for Grid Connected Plug-in Hybrid Electric Vehicles (PHEV)," in *Proceedings of IEEE Energy 2030 Conference on Global Sustainable Energy Infrastructure*. Atlanta, GA, USA: IEEE, November 2008, pp. 1–8.

[9] W. Kempton and J. Tomic, "Vehicle-to-Grid Power Fundamentals: Calculating Capacity and Net Revenue," *Journal of Power Sources*, vol. 144, no. 1, pp. 268–279, June 2005.

[10] J. C. Smith, R. Thresher, R. Zavadil, E. DeMeo, R. Piwko, B. Ernst, and T. Ackermann, "A Mighty Wind: Integrating Wind Energy into the Electric System is Already Generating Excitement," *IEEE Power & Energy Magazine*, pp. 41–51, March 2009.

[11] Z. Xu, M. Gordon, M. Lind, and J. Østergaard, "Towards a Danish Power System with 50% Wind: Smart Grids Activities in Denmark," in *Proceedings Power & Energy Society General Meeting*. IEEE Power Engineering Society, July 2009, pp. 1–8.

[12] L. Guzzella and A. Sciarretta, *Vehicle Propulsion Systems: Introduction to Modeling and Optimization*, 2nd ed. Berlin: Springer, 2007.

[13] L. Serrao, Z. Chehab, Y. Guezennec, and G. Rizzoni, "An aging model of Ni-MH batteries for hybrid electric vehicles," in *Proceedings of the Vehicle Power and Propulsion Conference*, Chicago, IL, 7–9 Sept 2005, pp. 1–8.

[14] Saft Batteries, "High Energy Lithium-Ion Cell VL 45 E Cell," Jan 2010, 54041_VL45E_cell_0305.61b6a847-bc8b-4fef-8a73-f196416b1758.pdf. [Online]. Available: http://www.saftbatteries.com

[15] A123Systems, "High Power Lithium Ion ANR26650M1A," Jan 2010, ANR26650M1A_Datasheet_APRIL_2009.pdf. [Online]. Available: http://www.a123systems.com

[16] *IBM ILOG CPLEX V12.1: User's Manual for CPLEX*, International Business Machines Corporation, 2009.